

Supporting Information

Controlled synthesis of $\text{CaTiO}_3:\text{Ln}^{3+}$ nanocrystals for luminescence and photocatalytic hydrogen production

Ling Meng, Kaifu Zhang, Kai Pan, Yang Qu* and Guofeng Wang*

Key Laboratory of Functional Inorganic Material Chemistry, Ministry of Education, School of Chemistry and Materials Science, Heilongjiang University, Harbin, 150080, P. R. China.

E-mail: copy0124@126.com; wanggf_w@163.com

Table S1. Effect of the $\text{Ca}(\text{CH}_3\text{COO})_2$ and $\text{Ti}(\text{OC}_4\text{H}_9)_4$ contents and reaction solvent on the compositions of samples. (a, b) direct dried in air at 180 °C for 24 h and sintered at 600 °C for 2 h. (c, d, e, f, g) after hydrothermal treatment at 180 °C for 24 h, dried in air at 80 °C for 4 h, and sintered at 600 °C for 2 h.

Samples	$\text{Ca}(\text{CH}_3\text{COO})_2$	$\text{Ti}(\text{OC}_4\text{H}_9)_4$	Reaction solvent (30ml)	Treatment	Production
(a)	1.321 g	1.7 ml	ethylene glycol	Sol-gol	$\text{CaTiO}_3 + \text{CaCO}_3$
(b)	1.175 g	1.7 ml	ethylene glycol	Sol-gol	$\text{CaTiO}_3 + \text{CaCO}_3$
(c)	0.882 g	1.7 ml	ethylene glycol	hydrothermal	$\text{CaTiO}_3 + \text{CaCO}_3$
(d)	1.763 g	3.4 ml	ethylene glycol	hydrothermal	$\text{CaTiO}_3 + \text{CaCO}_3$
(e)	0.882 g	1.7 ml	ethanol	hydrothermal	$\text{CaTiO}_3 + \text{CaCO}_3$
(f)	1.763 g	3.4 ml	ethanol	hydrothermal	$\text{CaTiO}_3 + \text{CaCO}_3$
(g)	0.882 g	1.7 ml	methanol	hydrothermal	$\text{CaTiO}_3 + \text{CaCO}_3$

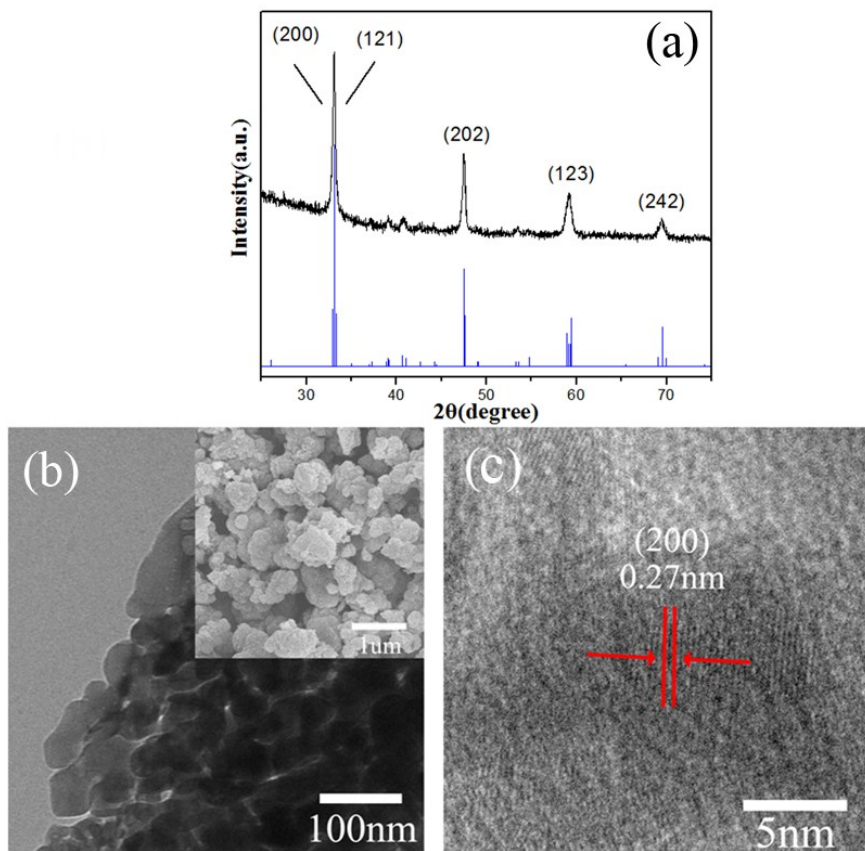


Figure S1. XRD patterns, SEM, TEM and HRTEM images of CaTiO_3 nanocrystals.

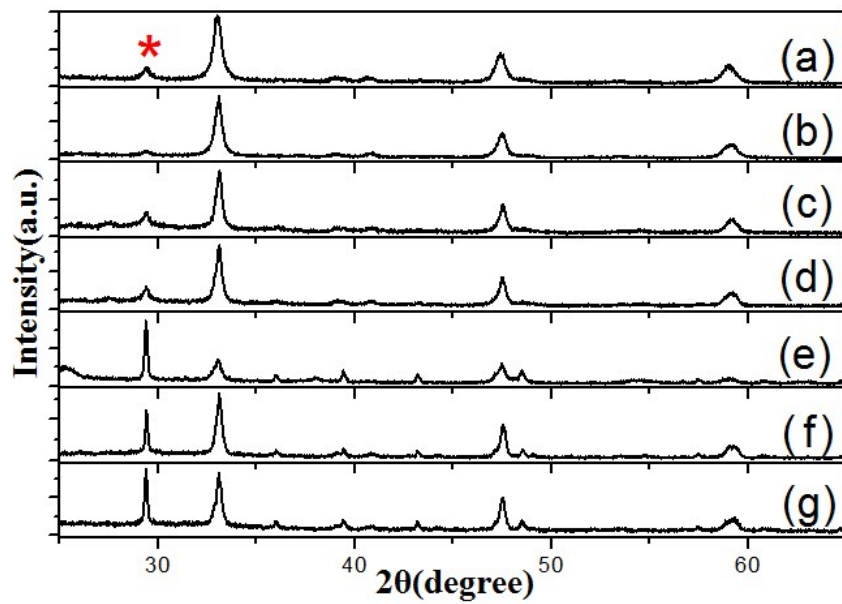


Figure S2. XRD patterns of samples prepared at different conditions (corresponding to the sample (a-g) of Table S1). The peaks marked by asterisk (*) arise from calcite CaCO_3 particles (JCPDS 05-0586).

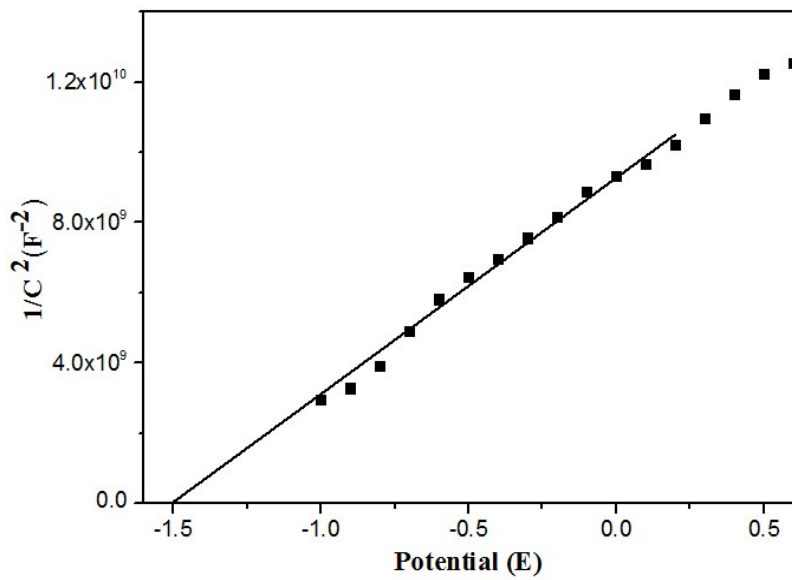


Figure S3. Mott–Schottky plots of CaTiO_3 nanocrystals.

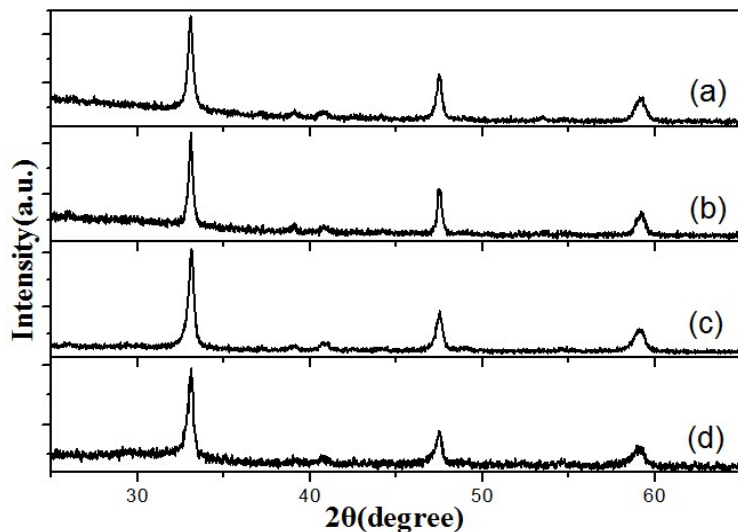


Figure S4. The XRD patterns of (a) $\text{CaTiO}_3:\text{Eu}^{3+}(0.5\%)$, (b) $\text{CaTiO}_3:\text{Eu}^{3+}(5\%)$, (c) $\text{CaTiO}_3:\text{Eu}^{3+}(15\%)$ and (d) $\text{CaTiO}_3:\text{Eu}^{3+}(20\%)$ nanocrystals.

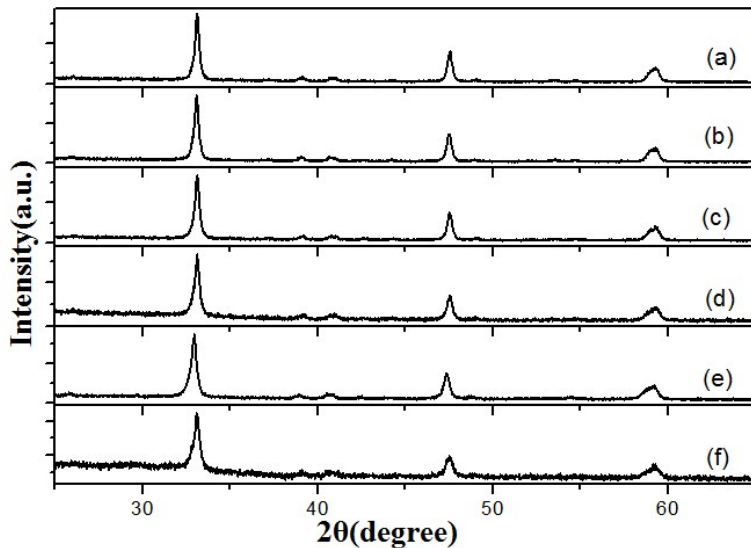


Figure S5. The XRD patterns of (a) $\text{CaTiO}_3:\text{Er}^{3+}(0.5\%)$, (b) $\text{CaTiO}_3:\text{Er}^{3+}(3\%)$, (c) $\text{CaTiO}_3:\text{Er}^{3+}(5\%)$, (d) $\text{CaTiO}_3:\text{Er}^{3+}(10\%)$, (e) $\text{CaTiO}_3:\text{Er}^{3+}(15\%)$ and (f) $\text{CaTiO}_3:\text{Er}^{3+}(20\%)$ nanocrystals.

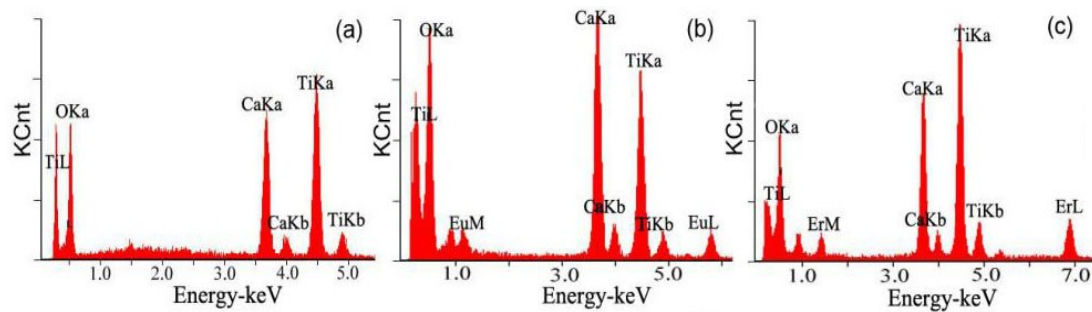


Figure S6. The EDX analysis results of (a) pure CaTiO_3 , (b) $\text{CaTiO}_3:\text{Eu}^{3+}(10\%)$, (c) $\text{CaTiO}_3:\text{Er}^{3+}(10\%)$ nanocrystals.

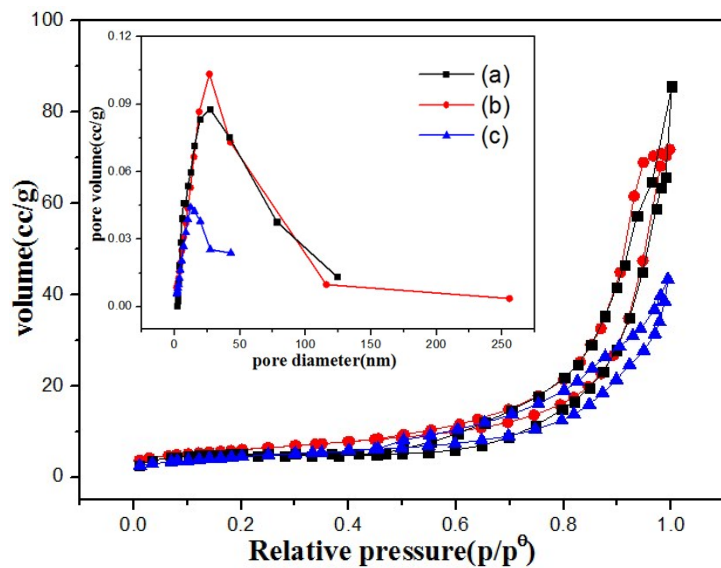


Figure S7. N₂ adsorption–desorption isotherm curves and pore size distribution (inset) of (a) CaTiO₃nanocrystals, (b) CaTiO₃:Er³⁺(0.5%), (c) CaTiO₃:Eu³⁺(0.5%)nanocrystals.